Characterizing the Impact of Interference through Spectral Analysis on Commercial 802.11 Devices

Kostas Chounos*, Stratos Keranidis*, Thanasis Korakis* and Leandros Tassiulas†
*Department of Electrical and Computer Engineering
University of Thessaly, Greece, Email: hounos,efkerani,korakis@uth.gr
†Department of Electrical and Computer Engineering
University of Yale, USA, Email: leandros.tassiulas@yale.edu

Abstract—**Performance experienced by end-users supporting the popular 802.11 protocol is significantly degraded in densely populated urban areas, mainly due to the extensive spectrum sharing and the resulting 802.11 impairments such as "hidden-terminals", overlapping channel interference, etc. Moreover, as the unlicensed spectrum is also home for other wireless technologies and a large range of RF devices, the experienced channel conditions further deteriorate due to cross-technology interference. While the various resulting phenomena can be efficiently mitigated by isolating affected links from interference sources over spectrum, 802.11 networks currently lack unified mechanisms for characterizing the impact of different interference sources across the available channel configurations. In this work, we take advantage of spectral measurements available at the PHY-layer of commercial 802.11 equipment, in order to develop a highly accurate spectral analysis mechanism that is able to quantify the impact of interference on WLAN performance. The developed distributed mechanism concurrently operates on all network nodes and characterizes the band of interest with minimal overhead. Through the implementation of our approach on commercial 802.11n chipsets and its detailed experimental evaluation, we showcase its applicability in characterizing the impact of spectrum congestion and interference in a unified way, towards driving efficient spectrum adaptation decisions.**

I. Introduction

The wide adoption of wireless networking technologies in everyday life scenarios has created unprecedented levels of congestion in unlicensed frequency bands. Core factors impacting spectrum congestion include the ever-increasing density of WLAN deployments, along with the limited availability of non-overlapping channels and the uncoordinated management of common setups. In this context, it is rather common for 802.11 networks to experience extensive sharing of spectrum resources with collocated links, thus providing fertile ground for the appearance of common 802.11 problems such as "hidden-terminals", channel overlapping etc. Consequently, the network performance experienced by 802.11 end-users in high density deployments is significantly degraded.

Spectrum in unlicensed bands is also being heavily utilized by other wireless protocols (e.g., Bluetooth, Zigbee) and a large range of RF devices (e.g. cordless phones, security cameras), or even Microwave ovens. Recent studies [1], [2] have shown that non-WiFi devices appear rather frequently and with fairly high signal strengths, resulting in strong cross-technology interference. Considering also that the concept of LTE in Unlicensed spectrum (LTE-U), originally proposed by Qualcomm in [3], has been officially included in the latest release 13 of LTE standard [4], we clearly understand that the unlicensed spectrum will keep becoming increasingly crowded with diverse technologies.

The aforementioned interference sources pose even more critical impact on deployments supporting the latest wireless standard versions, which adopt channels of wider width. More specifically, IEEE 802.11n [5] supports up to 40 MHz channels and the IEEE 802.11ac [6] further increases the channel width up to 160 MHz, in an effort to improve the achievable data rates. Nonetheless, while the throughput performance of high SNR links nearly doubles when doubling the configured bandwidth, this property no longer holds in the presence of interference as presented in [7], thus showing that fixed application of wider channel widths (as followed by 802.11n) is not the optimal solution. Towards achieving fair spectrum sharing with legacy devices and avoiding cross-technology interference, the 802.11ac protocol allows channel bandwidth to be determined on a frame-by-frame basis. In spite of the extra protection mechanisms that 802.11ac features for combating interference, detailed experimental results provided in the recent studies [8], [9] showcased that performance is prone to both 802.11 and heterogeneous transmissions on secondary channels. Taking into account the above, we clearly understand that careful interference management needs to be applied in accordance with planned selection of primary channels, in order to take advantage of the excess capacity that larger channel widths are able to offer.

In this work, we propose a spectrum evaluation approach that is able to quantify the impact of various interference sources on WLAN performance in a unified way. The offered wide applicability and ease of deployment consist the proposed solution ideal for careful planning of channel assignments, as well as for driving efficient spectrum adaptation decisions for 802.11ac networks in the long term.

A. Related Work

A large body of research studies has focused on accurately characterizing the spectrum utilization in ISM bands. The works in [10], [11] presented detailed spectrum occupancy evaluations of the ISM band over diverse scenarios, by utilizing high precision devices like spectrum analyzers. The authors in [12] developed a frequency adaptation algorithm that aims at maximizing the achievable capacity and implemented their approach on a Software Defined Radio platform.

On the other hand, the work in [1] presented the innovative Airshark system that builds on the spectral analysis capabilities of commodity WiFi hardware to provide identification of cross-technology interfering devices. Trying to address the common 802.11 problematic scenarios of ”hidden and exposed terminals”, the works in [13], [7] proposed approaches that resolve identified link conflicts through centralized scheduling, thus being applicable only to centrally managed WLANs.

Except from the aforementioned research approaches, several commercial frameworks provide ways of quantifying spectrum usage in ISM bands. More specifically, the Ubiquiti Air View [14] enables extraction of useful information about spectrum usage and representation through Power Spectral Density (PSD). The Air Magnet system [15] provides more sophisticated capabilities, such as interference classification and Duty cycle evaluation. The most comprehensive solution appears to be the Cisco MERAKI framework [16], which supports quantification of both 802.11 and heterogeneous spectrum utilization and utilizes these data to configure updated channel configurations in an automated way. The common downside of all the above commercial frameworks is that they either prerequisite the use of additional hardware or induce network downtime, while collecting measurements.

B. Our Contribution

In this paper, we propose and develop a spectrum occupancy evaluation framework that relies on spectral measurements to quantify the impact of interference on the performance of 802.11 links. The key novelty of the proposed solution is that it takes advantage from the inherent spectrum sensing capabilities of commercial 802.11 hardware, thus providing for rapid deployment on existing 802.11 equipment. Identification of 802.11 link conflicts is executed in a distributed way through detailed interpretation of spectral measurements at both the transmitter and receiver sides of each link. Building the proposed mechanism on generic metrics that interpret raw spectral data, we offer the ability to detect transmissions of non-802.11 devices, consisting our solution aware of cross-technology interference as well. Through extensive experimentation in realistic testbed deployments and across a wide range of interference sources and scenarios, we verified the perceived spectrum evaluation accuracy along with the wide applicability of the proposed solution. Finally, we also experimentally verified that the careful design and implementation of the overall framework resulted in minimal injected protocol overhead.

II. Proposed System

Through this work, we build on the inherent spectrum sensing capabilities of 802.11 hardware to develop a spectral analysis mechanism that is able to quantify the impact of interfering transmissions to 802.11 links. Considering that the link of interest uses a specific central frequency $\mathcal{F}_c$ and channel bandwidth $\mathcal{BW}$, we propose to quantify spectrum utilization between frequencies F_c - $BW/2$ and F_c + $BW/2$ at both the transmitter and receiver to associate this information with the channel conditions experienced at each side.

A. 802.11 Basics

According to the standard, 802.11 transceivers first employ the CSMA/CA procedure before initializing transmissions, in order to detect whether the detected Power level on $\mathcal{F}_c$ exceeds specified thresholds [17]. In the case where the detected power exceeds the Energy Detection (ED) threshold the medium is directly declared as busy, while in the case of power exceeding the lower Clear Channel Assessment (CCA) threshold and only if the 802.11 signal preamble is successfully decoded, the medium is defined to be busy. In both cases, transmissions are postponed to avoid collisions, while throughput performance is degraded proportionally to the amount of captured channel access time. On the other hand, if none of the above cases is satisfied, the medium is declared as idle and transmissions are allowed. However, the resulting throughput might still be degraded in the case that transmitted frames collide with other transmissions that are detected at high power levels at the receiver side. In this case, the probability of collisions depends on the amount of time captured by interfering nodes [18].

Based on the above observations, we aim at evaluating the amount of channel time captured at both the transmitter and receiver ends, in order to characterize how interference affects the protocol operation. To this aim, we employ the scanning capabilities of OFDM compatible hardware, as the 802.11 implements the OFDM scheme since the introduction of 802.11a and its posterior g, n and ac amendments. OFDM compatible receivers [19] feature hardware dedicated in implementing the Fast Fourier Transfer (FFT) algorithm, in order to convert received OFDM signals from time to frequency domain and feed data to the corresponding channel subcarriers $\mathcal{SC}$. This process includes the collection of a spectral sample $\mathcal{S}$ collected on $\mathcal{F}_c$, comprising the Power level received on each one of the $\mathcal{SC}$, and denoted by $\mathcal{P}(i, \mathcal{S}, \mathcal{F}_c)$, i $\in \mathcal{SC}$.

B. Spectrum Occupancy Evaluation

For the purposes of our evaluation, we decided to use the notion of *Duty Cycle* (DC) as the core metric for describing the percentage of time in which the Power of the considered spectrum fragment exceeds a specific Power Threshold $\mathcal{P}_{\mathcal{T}H}$. We use $\mathcal{P}(\mathcal{S}, \mathcal{F}_c, \mathcal{BW})$ to denote the power of Spectral Sample $\mathcal{S}$ that has been collected on the central frequency $\mathcal{F}_c$, characterises a total bandwidth of $\mathcal{BW}$ MHz wide spectrum and calculated it as:

$$\mathcal{P}(\mathcal{S}, \mathcal{F}_c, \mathcal{BW}) = \sum_{i}^{\mathcal{SC}} \mathcal{P}(i, \mathcal{S}, \mathcal{F}_c) \tag{1}$$

where $P(i, \mathcal{S})$ denotes the power at each corresponding subcarrier of spectral sample $\mathcal{S}$. We also use $\mathcal{N}_S$ to denote the amount of samples that have been collected during the scanning process and correspond to a given $\mathcal{F}_c$. As our solution considers varying $\mathcal{BW}$ levels, we use $\mathcal{D}C(\mathcal{F}_c, \mathcal{BW})$ to denote the *Duty Cycle* of the spectrum part between frequencies F_c - $BW/2$ and F_c + $BW/2$ and calculate it as follows:

$$\mathcal{D}C(\mathcal{F}_c, \mathcal{BW}) = \frac{1}{\mathcal{N}_S} \sum_{S=1}^{\mathcal{N}_S} on(\mathcal{P}(\mathcal{S}, \mathcal{F}_c, \mathcal{BW}), \mathcal{P}_{\mathcal{T}H}) \tag{2}$$

where the function $on(\mathcal{P}(\mathcal{S}, \mathcal{F}_c, \mathcal{BW}), \mathcal{P}_{\mathcal{T}H})$ is equal to 1 if the $\mathcal{P}(\mathcal{S}, \mathcal{F}_c, \mathcal{BW})$ of the spectral sample under consideration exceeds the $\mathcal{P}_{\mathcal{T}H}$ threshold, and 0 otherwise.

There is a huge amount of works related with the definition of appropriate detection thresholds. However, as our system

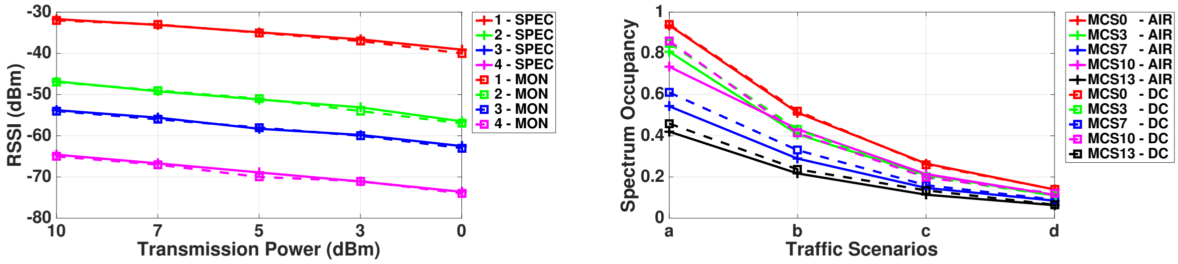

(a) RSSI

(b) Spectrum Occupancy

Fig. 1: Initial Experiments for verifying detection accuracy

follows the standard 802.11 CSMA implementation, the CCA and ED thresholds as specified for each protocol version play the key role in performance (Table I). More specifically, when estimating channel conditions at the transmitter side, we need to consider either the CCA for evaluating the amount of captured channel time by decodable 802.11 transmissions or the lower ED threshold for non-decodable 802.11 or non-802.11 transmissions. On the other hand, at the receiver side our evaluation takes into account only the higher CCA threshold as any signal exceeding this value is potential interference.

Channel Width	CCA (primary)	CCA (non-primary)	ED
20MHz(n)(ac)	-82dBm	-72dBm	-62dBm
40MHz(n)(ac)	-79dBm	-72dBm	-59dBm
80MHz(ac)	-76dBm	-69dBm	-56dBm

TABLE I: IEEE 802.11 CCA and ED Thresholds

C. Implementation

Several commercial 802.11 devices (supporting the n and ac standards) developed by major vendors of wireless products, such as Qualcomm and Intel, provide access to raw spectral samples through interfaces implemented in Open-Source drivers (ath9k [20], iwlwifi [21], and ath10k [22], etc.). In this work, we employ the commercial Qualcomm AR9380 802.11n compatible chipset [23] that is 3x3 MIMO and supports the 20 MHz and 40 MHz channel widths and control it over the ath9k driver. The default ath9k implementation supports a background scanning mechanism at the station mode of operation, which scans the list of available 20 MHz channels for discover neighboring APs. Collection of spectral samples runs also in parallel over the list of channels accessed through the background scanning. The AR9380 remains on each channel for the scanning interval of $\sim$50 ms and supports the maximum sampling rate of $\sim$100 KSps, featuring also a relatively low channel switching delay of $\sim$1-2 ms.

In order to scan the 2.4 GHz ISM band of interest that is 80 MHz wide, we need to manually execute it at least 4 times for steps of 20 MHz. Through tests, we observed that the AR9380 is able to efficiently store up to 250 spectral samples per scanned channel. While the sample collection procedure might end much sooner than the scanning interval, given the configured sampling rate and number of samples, the card will still remain on the channel. In order to decrease the overall overhead of the scanning operation, we decided to decrease the channel interval from 50 ms down to 15 ms, taking into account that the maximum signal under consideration would be the emission of MW ovens that lasts $\sim$ 8.8 ms. Moreover, we configured the sampling rate of 16.67 KSps, so that the collected samples are equally distributed over the scanning interval of 15 ms. Having significantly reduced the overall scanning overhead, we also decided to scan in steps of 10 MHz, so that we decrease the spectrum separation between the configured $\mathcal{F}_c$ and the detected signals. Thus we require 7 operations starting from frequency 2412 MHz and ending on 2470 MHz for covering the 80 MHz. Through extra driver modifications, we ported the above procedure at the AP side as well and also configured it to take place simultaneously at both sides, by utilizing Beacon timestamps for synchronization. The collected spectral samples across the whole band are subsequently fed to an external program written in C that interprets them in detailed Received Signal and Duty Cycle measurements, as described through equations (1), (2). As our implementation is based on 802.11n, we use the corresponding CCA and ED thresholds of -82 dBm and -62 dBm. We also verified the successful operation of our solution on the 802.11ac Qualcomm AR9880 chipset using ath10k driver.

III. Initial Experiments

The detailed experimental evaluation that follows has been executed on the NITOS [24] indoor testbed that provides a wide range of wireless hardware in an interference-free environment. This first set of experiments focuses on validating the spectrum evaluation accuracy of the proposed mechanism across both 802.11 and cross-technology signals.

A. 802.11 signal detection

The experimental setup includes four different 802.11n 20 MHz links ranging from high-SNR to low-SNR, which are also configured across five different Transmission Power values to transmit backlogged traffic using MCS 0. We use an extra node that operates in Monitor mode and an external Python script to log the RSSI of all received packets and compare it with the average Received Signal as estimated through equation (1) over the spectral data captured at the same node. In Fig. 1(a), we observe the perceived accuracy of our Received Signal estimation across a wide range of link SNRs.

Next, we focus solely on the high-SNR link and configure it to use 5 different MCS configurations (0, 3, 7, 10, 13) and also four different application-layer traffic loads to vary the occupied channel airtime. The same node is used to sniff all transmitted packets and calculate the occupied channel time through the Python script by aggregating the duration of each captured frame. Fig. 1(b) presents the collected results and verifies the accuracy of the DC estimation. More specifically, we observe that for the MCS 0 scenario the DC closely approximates the channel airtime, while the deviation slightly increases for higher MCSs with the maximum value

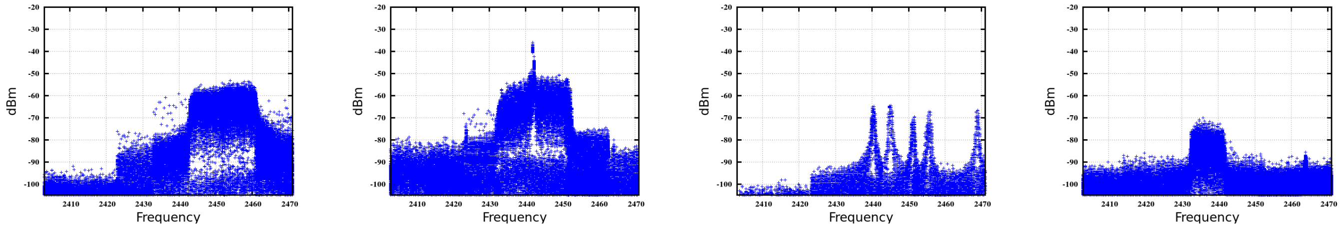

(a) 802.11n - 20 MHz (b) Microwave oven (c) Bluetooth 4.0 (d) LTE-U

Fig. 2: PSD as evaluated during the operation of each different RF device

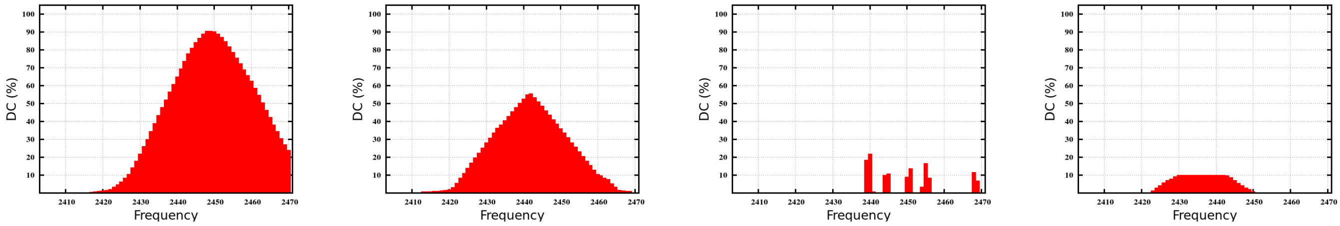

(a) 802.11n - 20 MHz (b) Microwave oven (c) Bluetooth 4.0 (d) LTE-U

Fig. 3: Duty cycle as evaluated during the operation of each different RF device

measured to be ∼12% for the highest load of MCS 10. Having verified the accuracy of detecting 802.11 transmissions, we next proceed by experimenting with signals of heterogeneous technologies.

B. Cross-technology signal detection

For this purpose, we generate transmissions through different types of RF hardware to characterize the resulting PSD and DC evaluation over the 2.4 GHz band. More specifically, we use an 802.11n link that transmits saturated traffic at MCS 7, a Bluetooth 4.0 dongle, while we also configure a USRP B210 [25] to emulate the signal transmitted by a Microwave oven and an LTE-U femtocell. To setup the LTE-U eNodeB device, we use the opensource srsLTE framework [26]. During the operation of each different device, we plot the PSD as captured by our sensing mechanism in Figures 2(a), 2(b), 2(c) and 2(d), while Figures 3(a), 3(b), 3(c) and 3(d) depict the DC evaluation. We clearly observe the high spectrum utilisation (∼90%) that 802.11n links are able to achieve at high AMPDU aggregation sizes, along with the precise detection of the DC of microwave ovens that typically emit high RF energy in 2.44-2.47 GHz frequencies with DC of ∼50%, as mentioned in [1]. Moreover, we are also able to capture transmissions of the Bluetooth that performs frequency hopping and efficiently detect spectrum fragments, on which the frequency hopping devices operate less frequently. In Fig. 3(c), we depict the DC evaluation when considering channels of 1 MHz width, as channels 20 MHz presented zero DC. Our observations agree with other cross-technology interference related studies [1], [2] that characterize Bluetooth as a light interference source that only minimally affects the performance of 802.11 links, due to its relatively low transmission power. The emulated LTE-U device implements the eNodeB, utilizing 10 MHz of bandwidth and transmitting System Information Broadcasting messages over the Physical Broadcast Channel (PBCH) [4]. Though the DC evaluation, we notice the remarkably high signaling overhead of ∼10% that is used by LTE systems for broadcasting purposes.

IV. Experimental Evaluation

In this section we present a thorough analysis of 802.11 problematic scenarios through the proposed approach. We deploy our mechanism on an 802.11n link (referred as System under Test - SUT) and use another 802.11n link as the interference source (referred as Interferer - INT). More specifically, we experiment with ”hidden-terminal” and adjacent channel interference scenarios. Taking advantage of detailed statistics exposed by the ath9k driver, we also log the MAC layer Packet Delivery Ratio (PDR) performance, for aiding in interpretation of experimental results.

A. Hidden-terminals

For the purposes of this experiment, we configure two links that appear to be hidden to each other. More specifically, the INT link appears to be hidden to the transmitter of the SUT link while the receiver is directly impacted by INT transmissions. We verify this claim, by ensuring that the SUT transmitter cannot decode any frames of the INT link when sniffing in Monitor mode. On the other hand, the INT link is constantly not affected by the SUT transmissions, thus enabling us to focus solely on analyzing the performance of the SUT link. We configure the SUT to use the fixed MCS 0, while generating different scenarios for the INT link by using both MCS 0 and MCS 7 and varying the injected application layer traffic load as well.

By applying our spectrum evaluation mechanism, we first verify that the INT link appears hidden to the SUT transmitter as it detects zero DC. However, the throughput results of Fig. 4(a) present remarkably low performance especially under high traffic conditions for the INT link. Fig. 4(c) presenting the DC as measured at the SUT receiver, clearly highlights that the performance degradation is only attributed to receiver side interference, which is also verified by the low PDR, as shown in Fig. 4(b). Taking a closer look at the results, we observe that the DC evaluation is inversely proportional and complementary to the throughput and PDR performance, across the range of tested scenarios. This is expected as in this setup every collision event results in frame losses only

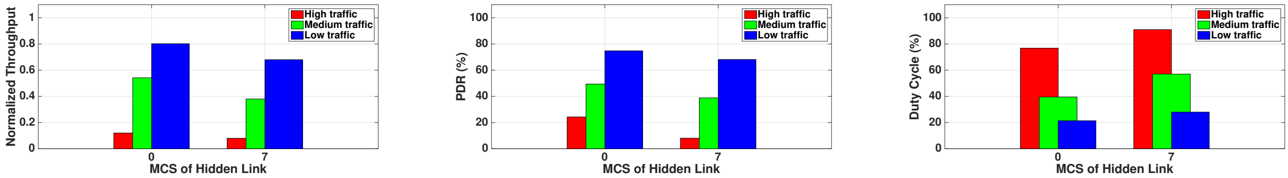

(a) Throughput (b) PDR measured at the receiver (c) DC measured at the receiver

Fig. 4: Hidden-terminal scenarios - Performance of SUT link

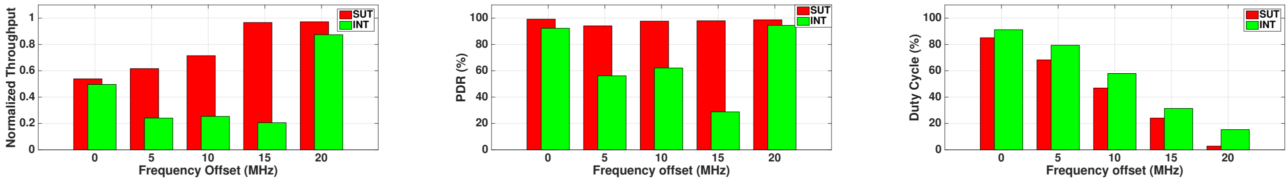

(a) Throughput (b) PDR measured at the transmitter (c) DC measured at the transmitter

Fig. 5: Adjacent channel interference scenarios - Performance of both SUT and INT links

for the SUT link and as a result affects PDR and throughput proportionally. The key outcome of this experiment is that even difficult to handle 802.11 impairments can be easily identified through joint interpretation of spectral measurements at both the transmitter and receiver sides.

B. Overlapping channel interference

In this experiment, we use two high-SNR 802.11n links with closely spaced ($\sim$5m) transmitter-receiver pairs. By measuring both link strengths, we remark that the SUT link approximates the -37 dBm and the INT link the -45 dBm. Since both links are able to sense each other's transmissions, the medium is fairly shared when operating on the same channel, thus highlighting the impact of channel contention. Next, we gradually tune the frequency of one link (INT) in steps of 5 MHz to increase the frequency offset between their central frequencies.

Fig. 5(a) and 5(b) depict the performance of both the SUT and INT links in terms of throughput and PDR accordingly, while Fig. 5(c) shows the DC measurements as evaluated at the transmitter of each link. Due to the close proximity between the transmitter-receiver pair of both links, their DC measurements appear to be identical and for this reason we present only the transmitter side evaluation. Focusing on the case where the same frequency is configured, we observe that both links detect DC values close to 90% and approximately equally share throughput. This observation comes due to the fact that during the spectral data collection procedure, lasting for 15 ms, the contending link experiences undisturbed access to the medium, thus resulting in high DC measurements.

In scenarios of increasing frequency offset separation (moving from 5 MHz to 15 MHz), the DC evaluation shows that the links no longer share the medium equally, estimating higher performance for the SUT link that detects lower DC values. Moreover, we observe that the SUT link gradually improves the obtained throughput as the impact of overlapping channel interference decreases. On the other hand, the INT link achieves constantly much lower throughput compared to SUT, while it also detects decreasing DC values between 5 MHz to 15 MHz separation. In an effort to detect the cause, we focus on PDR performance, which shows constantly lower performance for INT link in comparison with the SUT, clearly showing that the SUT link captures the channel, as a consequence of its higher signal strength compared to INT link. In the case of 20 MHz channel separation (no overlap), both links experience nearly isolated operation reaching close to maximum nominal throughput. Concluding, we observed that the proposed spectrum evaluation procedure enabled both links to detect ongoing transmissions on overlapping channels and quantify the impact of adjacent channel interference to understand whether it affects them or not. However, we remark that the joint impact of "capture effect" further complicates the channel sharing process, and motivates further investigation.

C. Outdoor experiments

In this experiment, we deploy our spectrum sensing solution in an outdoor located densely populated area, in the city center of Volos, Greece. The monitoring device is placed on the 3rd floor of an open space offices building that faces a park. We collect spectral measurements every 5 seconds and evaluate the utilization through the DC metric on a 24/7 basis. Fig. 6(a) and 6(b) correspond to measurements collected over 4 weeks and illustrate the maximum spectrum occupancy per hour of day and the average occupancy over channels 1-11 accordingly. We can see that the lowest utilization appears between 00:00-08:00, while much higher values are observed between 08:00-23:00. In addition, lower utilization is indicated during the weekends, in comparison with weekdays. Results presented in Fig. 6(b) demonstrate unequal distribution of traffic across channels, with channels 5-7 being far more utilized than channels 1 and 2. These measurements showcase the advantage of employing the proposed solution for planning of channel assignments.

D. Overhead Consideration

Parameters affecting the overall induced overhead include the number of central frequencies to be scanned, the scanning interval and scanning period (SP), as well as the overhead injected during channel switching. Having described the exact values configured in our implementation (Section II.c), in this experiment we vary the period over which scanning procedures are executed that exerts crucial influence on the system performance between 100ms and 3 sec. To evaluate the injected overhead, we experiment with 5 different common traffic scenarios corresponding to VoIP calls and HD Video

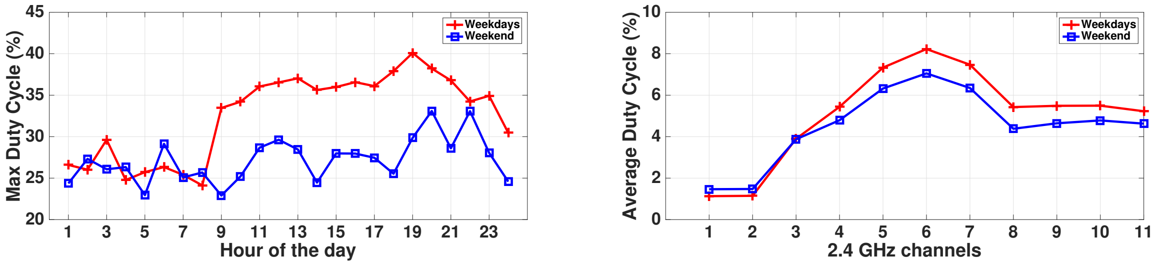

(a) Maximum Spectrum Occupancy over time

(b) Average Spectrum Occupancy per channel of the 2.4 GHz band

Fig. 6: Monitoring activity in outdoor environments

Streaming presented in Table II. The bandwidth requirements have been carefully selected to match the requirements specified by Skype [27] and Netflix [28] accordingly. Considering that during the overall band scanning procedure, our implementation provides intervals for regular traffic exchange, we do not expect higher layer protocols to be remarkably impacted by the introduced mechanism. Fig. 7 illustrates the nominal throughput obtained in each scenario and clearly shows that even extreme scanning period values of 100 ms only minimally impact performance. Based on the obtained results, we observe SP values between 1 and 3 sec that can provide the ideal trade-off between frequency of channel conditions updating and protocol overhead. For the sake of clarity, we remark that all the experiments presented prior to this section used the SP of 5 secs, in order to make sure that the scanning frequency did not affect the obtained results.

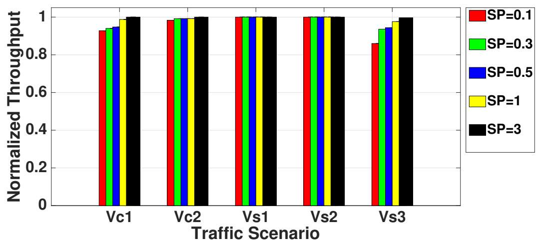

Fig. 7: Overhead evaluation

	Bandwidth
Video call Standard quality - Bi-directional (Vc1)	400Kbps
Video call High Definition - Bi-directional (Vc2)	1.2Mbps
Video Streaming Standard quality (Vs1)	3Mbps
High definition Video (Vs2)	5Mbps
Full High definition Video (Vs3)	25Mbps

TABLE II: Throughput Demands

V. Conclusions and Future Work

In this work, we presented a comprehensive framework that relies on spectrum analysis for quantifying the interference impact on 802.11 links. The proposed mechanism takes advantage of PHY-layer measurements available on standard compliant 802.11 hardware. An extensive experimental study of the proposed system's operation under different interference sources was presented. As part of our future work, we aim at evaluating the performance gains of 802.11ac systems when adapting the frequency and bandwidth parameters by utilizing the developed spectrum evaluation procedure.

VI. Acknowledgments

We would also like to thank our colleagues Ilias Syrigos and Virgilios Passas who provided insight and expertise that greatly assisted in the resulting research.

References

[1] S. Rayanchu, A. Patro, and S. Banerjee. Airshark: Detecting non-WiFi RF Devices Using Commodity WiFi Hardware. In *Proceedings of IMC*, 2011.

[2] S. Gollakota, F. Adib, D. Katabi, and S. Seshan. Clearing the RF Smog: Making 802.11N Robust to Cross-technology Interference. In *Proceedings of SIGCOMM*, 2011.

[3] Qualcomm. Extending the Benefits of LTE to Unlicensed Spectrum. In *LTE in Unlicensed Spectrum workshop, Paris, France*, 2014.

[4] *"Evolution of LTE in Release 13"*, http://www.3gpp.org/news-events/3gpp-news/1628-rel13.

[5] IEEE 802.11n-2009, Amendment 5: Enhancements for Higher Throughput., 2009.

[6] IEEE 802.11ac-2013, Amendment 4: Enhancements for very high throughput for operation in bands below 6 GHz., 2013.

[7] S. Rayanchu, V. Shrivastava, S. Banerjee, and R. Chandra. FLUID: Improving Throughputs in Enterprise Wireless Lans Through Flexible Channelization. In *Proceedings of MOBICOM*, 2011.

[8] Y. Zeng, P. H. Pathak, and P. Mohapatra. A first look at 802.11ac in action: Energy efficiency and interference characterization. In *Proceedings of IFIP*, 2014.

[9] M. D. Dianu, J. Riihijrvi, and M. Petrova. Measurement-Based Study of the Performance of IEEE 802.11ac in an Indoor Environment. In *Proceedings of ICC*, 2014.

[10] M. Lpez-Bentez and F. Casadevall. Spectrum Occupancy in Realistic Scenarios and Duty Cycle Model for Cognitive Radio. *Advances in Electronics and Telecommunications*, 1(1), apr 2010.

[11] M. Cardenas-Juarez, M. A. Diaz-Ibarra, U. Pineda-Rico, A. Arce, and E. Stevens-Navarro. On spectrum occupancy measurements at 2.4 ghz ism band for cognitive radio applications. In *Proceedings of CONIELECOMP*, pages 25–31, Feb 2016.

[12] J. Bajaj, W. Kim, S. Y. Oh, and M. Gerla. Cognitive radio implementation in ism bands with microsoft sora. In *Proceedings of PIMRC*, pages 531–535, Sept 2011.

[13] V. Shrivastava, N. Ahmed, S. Rayanchu, S. Banerjee, S. Keshav, K. Papagiannaki, and A. Mishra. Centaur: Realizing the full potential of centralized wlans through a hybrid data path. In *Proceedings of Mobicom*, 2009.

[14] *"Ubiquiti Air View"*, https://help.ubnt.com/hc/en-us/articles/204950584-airMAX-How-to-use- airView-to-find-the-best-channel.

[15] *"Air Magnet Spectrum XT"*, http://www.flukenetworks.com/enterprise-network/wireless-net- work/airmagnet-spectrum-xt.

[16] *"Cisco Meraki"*, https://documentation.meraki.com/MR/Radio.

[17] IEEE 802.11-2007 Wireless LAN Medium Access Control and Physical Layers Specifications., 2007.

[18] G. Bianchi. Performance analysis of the IEEE 802.11 distributed coordination function. *Selected Areas in Communications, IEEE Journal on*, 18(3):535–547, March 2000.

[19] T.H. Meng, B. McFarland, D. Su, and J. Thomson. Design and implementation of an all-CMOS 802.11a wireless LAN chipset. *Communications Magazine, IEEE*, 41(8):160–168, Aug 2003.

[20] *"Ath9k - Driver 802.11n"*, https://goo.gl/HKm830.

[21] *"Iwlwifi - Intel Driver 802.11n"*, https://goo.gl/BrKK7c.

[22] *"Ath10k - Driver 802.11ac"*, https://goo.gl/vq8hF6.

[23] *"Qualcomm AR9380 Chipset"*, http://goo.gl/51Mg7.

[24] *"NITOS testbed"*, http://nitlab.inf.uth.gr.

[25] *"USRP B210"*, https://www.ettus.com/product/details/UB210-KIT.

[26] *"srsLTE - open-source LTE library"*, https://github.com/srsLTE/srsLTE.

[27] *"Skype Bandwidth Requirements"*, https://goo.gl/BdjbKk.

[28] *"Netflix Bandwidth Requirements"*, https://goo.gl/5kycyS.